NANO LETTERS

2004
Vol. 4, No. 12
2513−2517

Percolation in Transparent and Conducting Carbon Nanotube Networks

L. Hu, D. S. Hecht, and G. Grüner*

Department of Physics and Astronomy, University of California Los Angeles, Los Angeles, California 90095

Received September 23, 2004; Revised Manuscript Received October 7, 2004

ABSTRACT

Ultrathin, uniform single-walled carbon nanotube networks of varying densities have been fabricated at room temperature by a vacuum filtration method. Measurements of the sheet conductance as a function of nanotube network density show 2D percolation behavior. In addition, the network transparency in the visible spectral range was examined and the results are in agreement with a standard thin-film model: fits to the standard theory indicate $\hat{U}_{ac} = \hat{U}_{dc}$ for transmission measurements at 550 nm. Transmission measurements also indicate the usefulness of nanotube network films as a transparent, conductive coating. Avenues for improvement of the network conductance are discussed.

Since their discovery in the early 1990s, single-walled carbon nanotubes (SWNTs) have been exhaustively researched, and still only the surface of their potential has been scratched. Their usefulness in applications stems from their amazing physical properties: single tube devices have mobilities as high as 100,000 cm^2/Vs,[1] current carrying capacities of 10^9 A/cm^2 (ref 2), and ON/OFF current ratios as large as 10^5.[3] However, applications using single nanotube devices, though superior in some aspects, have the major flaw of irreproducibility. It is difficult to reproduce single tube devices consistently due to the variations in chirality and geometry from tube to tube. However, in a nanotube network (NTN), the effects due to such individual variations are suppressed by the ensemble averaging over a large number of tubes. Therefore, NTNs can be reproducibly mass produced, and done so at low cost and high efficiency, making them ideal for applications. NTNs have already been extensively studied as thin-film transistors,[4,5] diodes,[6] field-activated optical modulators,[7] strain[8] and chemical sensors,[9] field emission devices,[10,11] and transparent conductive coatings.[7] We,[12] and another group,[13] have shown that a NTN containing a significant number of both metallic and semiconducting nanotubes can operate as the conducting channel in a field effect transistor (FET) configuration.

We have focused on two fundamental physical properties of NTNs: DC conductivity and optical transparency. In particular, for the former case, we have explored the DC conductivity of the film as the density (nanotubes/area) changes from a rare, submonolayer network, to a thick film. This falls under the marquee of percolation theory,[14−16] which studies the formation of conducting pathways in different dimensions, using objects of various geometries. One model uses a random array of long conducting sticks to study the formation of conducting channels across a material. Our data is in good agreement with predictions made by this particular percolative model and expands on previous studies of percolation behavior for nanotube-composite films.[17−19] Complementing the percolation studies, we have measured the transparency of these NTNs in the visible spectral range. Our findings show agreement with prior optical studies[20] and reveal that NTNs have potential applications as transparent, conductive coatings, with properties comparable to, yet below, indium tin oxide (ITO), which is the current industry standard.

There are several methods for fabricating nanotube films, including drop casting from solvents,[21] spin coating[4] and quasi-Langmuir−Blodgett deposition[22] for isotropic films, and dip-casting,[23] Langmuir−Blodgett deposition,[24] and gas flow cells[25] for oriented films. These methods can lack, however, film homogeneity and uniformity, efficiency of film production, film thickness controllability, and can be subject to flocculation due to van der Waals interactions between nanotubes. To produce uniform films of single-walled nanotubes, we used a vacuum filtration method that involves vacuum filtering a dilute suspension of nanotubes in a solvent over a porous alumina filtration membrane (Whatman, 20 nm pore size, 47 mm diameter). For our experiment, purified HPCo nanotubes (average diameter 2 nm; average length 2 um) were sonicated in chloroform for 30 min to dissolve and debundle the nanotubes, making a solution with 0.2 mg NT per liter of chloroform. This solution was then quickly vacuum filtered through a 60 μm thick alumina membrane (time scale of a few seconds). As the solvent falls through the pores, the nanotubes are trapped on the surface of the filter, forming an interconnected network. The density of this

* Corresponding author. E-mail: ggruner@ucla.edu.

10.1021/nl048435y CCC: $27.50
Published on Web 10/22/2004

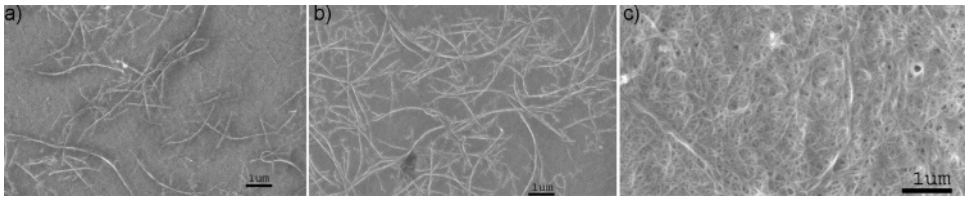

Figure 1. SEM images of the NTNs on alumina substrates, taken at 1.5 kV and 5 μA emission current. (a) Network resulting from filtering 7 mL of NT solution through the membrane. The filter pores are not visible in the scale shown. The network is near the percolation threshold and has few or no percolative paths through the sample. (b) 10 mL of NT solution for this sample. The network is above the percolation threshold and has several parallel pathways, allowing conduction across the film. (c) Film resulting from 400 mL of solution. Film is several layers thick.

network (nanotubes/area) can be controlled with high precision by simply controlling the volume of dilute suspension filtered through the membrane. Our method also has the benefit that the speed of the vacuum filtering process does not allow for tube flocculation, creating optically homogeneous films. Another factor that aids in homogeneity is that the denser regions act as a blockade to fluid flow through the filter, allowing rarer regions to accumulate tubes. The method is inexpensive, scalable to large areas, and allows for the transfer of the film to other surfaces by membrane dissolution.[7]

Figure 1 shows SEM images of three different samples (a, b, and c) that have been prepared by filtering a volume of 7 mL, 10 mL, and 400 mL, respectively, through the alumina. Several features can be noted in these images. First, though not shown here, images taken at various spots along the filter, sometimes separated by as much as 1 cm, show no noticeable difference in film characteristics, indicative of the spatial uniformity of the film. Also, the nanotubes appear randomly oriented with no preferential directions, allowing application of the percolation theory of a random distribution of conducting "sticks." Notice, however, that in these networks, each "stick" is actually a small bundle of nanotubes, because nanotubes tend to be attracted to each other through van der Waals interactions. We count each bundle of nanotubes as one "conducting stick" (CS). Percolation theory requires only that the CS has a length that is much greater than its diameter (the aspect ratio of the bundles is still of order 100). By manually counting the number of CS present in several images, we arrive at the average density (CS per area) for $V = 7$ mL is 1.2 CS/um^2 and $V = 10$ mL is 1.7 CS/um^2. As expected, the CS density is proportional to the volume of solution applied to the filter; i.e., if more nanotubes are used, a denser film results. Using this fact, the volume of NT solution used to make each filter can be directly converted into a CS density, using the conversion factor of 0.17 CS/ μm^2 mL.

Before measuring the DC conductivity of the NTN in the percolation region, we verified that all resistances measured were due to the nanotubes in the network and not due to the gold/nanotube interface at the contacts. To measure the contact resistance, different sets of gold contacts were evaporated onto the same filter, varying only the separation distance between the contacts (width between contacts held constant at 3 mm). The resistance between contacts of different channel length was then measured, and plots made

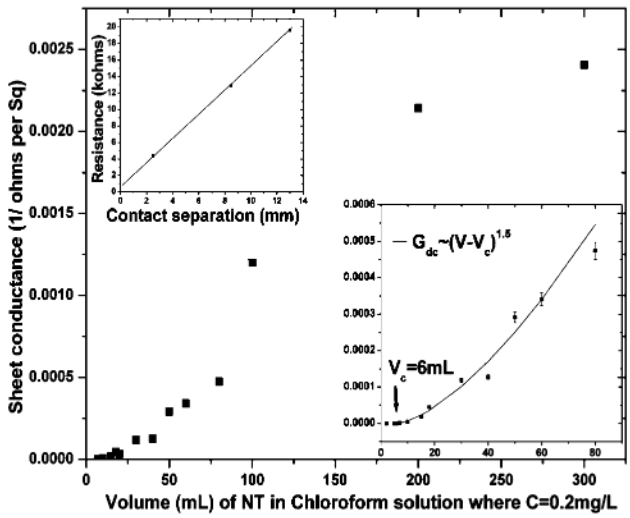

Figure 2. Sheet conductance vs volume of NT in chloroform solution. Notice the onset of conduction when the first percolative path across the sample is formed, indicated by $V_c = 6$ mL on the lower right inset. This inset shows the power fit in the percolation region, where the critical exponent $\alpha = 1.5$. Outside of the percolation region one starts to enter a linear regime. The inset in the upper left is the measured network resistance versus the source−drain distance, for networks of the same density.

of the resistance vs the contact separation; a typical plot is shown on the left upper inset of Figure 2. The plot shows a y-intercept (resistance at zero channel length) 8 times smaller than the resistance of the network at 3 mm channel length, the typical length used in our DC percolation measurements. This indicates that the resistance is dominated by the nanotube network, with only small contributions from the gold/nanotube interface at the contacts.

For the percolation study, several samples were made on identical filters, varying only the volume of solution (and therefore the NTN density). After the samples were prepared, identical gold contacts were evaporated to produce a NT channel 5 mm in width (W) and 3 mm in length (L). A standard two-probe measurement was made to measure the DC resistance (R) between the two gold contacts. To make comparisons with other work, resistance was converted to sheet resistance ($R_\square$), which is defined $R_\square = R(W/L)$. Figure 2 shows a plot of sheet conductance G (defined as $1/R_\square$) vs volume of the solution filtered through the alumina membrane (proportional to NT density).

Standard percolation theory predicts that the density dependence of the conductivity is given by

$$\sigma \propto (N - N_c)^{\alpha} \tag{1}$$

Here, σ refers to the conductivity in three dimensions and the sheet conductance G in two dimensions, N is the CS density, and N_c is the critical density corresponding to the percolation threshold. For the random distribution of the CS model,[14] the critical density is given by

$$l\sqrt{\pi N_c} = 4.236 \tag{2}$$

Here, l is the length of the CS. Equation 1 holds close to the transition; while well above the critical density, one expects to enter a region of linear dependence on density. The critical exponent, α, depends only on the dimensionality of the space; for a film in two dimensions, theory predicts $\alpha = 1.33$, while in three dimensions $\alpha = 1.94$.[26] The lower right inset of Figure 2 shows a fit of eq 1 to our data in the percolation region, using a critical volume value of 6 mL. The best fit to our data yields an experimentally measured value of $\alpha = 1.5$, which is close to but somewhat higher than theory predicts. There are several reasons why the measured and theoretical values would differ. First, critical exponents hold in the limit that one approaches the critical point. Since our measurement must encompass a range of points around the critical point, the exponent is not guaranteed to be exactly 4/3. In fact, as we approach the critical point, including fewer and fewer points in our fit, the exponent converges to 4/3. Discrepancies may also arise because our nanotube film is not perfectly two-dimensional, and one could be observing some crossover into three dimensions, where the critical exponent (α) is 1.94. Theory also does not account for the fact that both metallic and semiconducting nanotubes contribute to the conducting paths that are formed, with twice as many semiconducting as metallic tubes. The resistance of metallic−metallic tube interconnects has been shown to be less than the resistance of metallic−semiconducting junctions, due to the presence of a Schottky barrier.[27] In rare networks, the probability of all metallic tube paths is quite low, so that the conductance is limited by the Schottky barriers. However, as the network density increases, more pathways involving all metallic tubes are formed, yielding an increase in conduction with film density that is not accounted for by standard theory. We note that prior experiments on nanotube composites in three dimensions found α values of 1.2[28] and 1.3,[29] which are substantially different compared to theoretical prediction of $\alpha = 1.94$.

For the CS model of a random distribution of sticks, theory predicts the value of the critical density N_c, given as eq 2. Assuming an average nanotube length of 2 um (verified by SEM images), we calculate a theoretical critical density of 1.43 CS/μm^2. Using the data we obtain by counting the SEM images of films made at the critical volume of 6−7 mL, we measure a density of 1.2 CS/μm^2 at the critical point. The discrepancy between the data and theory can be accounted for by counting errors, or by nanotubes on the film that are not resolvable by the SEM, thus causing undercounting of the CS density.

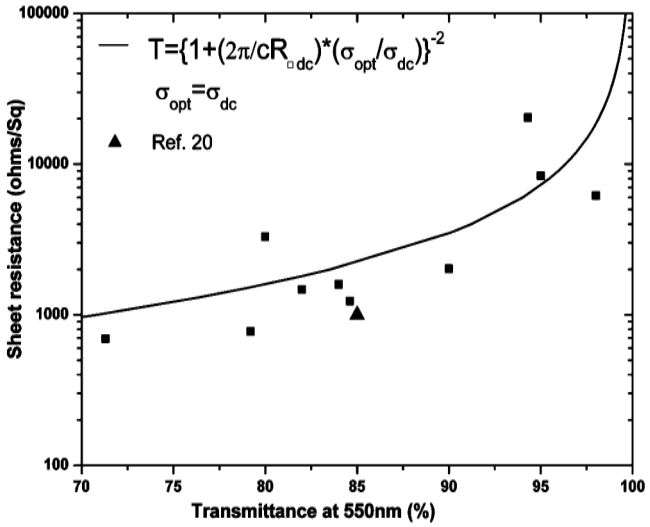

Figure 3. Transmittance at 550 nm for NTNs of various sheet resistances. The solid line is a fit to eq 3. We find that $\sigma_{ac} = \sigma_{dc}$ provides the best fit for the NTN data. Our data are in agreement with data provided by Manohar et al.

For NTNs that are on the conductive side of the percolation threshold, a possible application exists in the area of transparent, conductive coatings. We have evaluated the optical transparency, defined as the measured ratio of the transmitted and incoming radiation power at a chosen wavelength (our data is presented at 550 nm, for comparison with previous work). For the visible spectrum transmission data, a Beckman Coulter DU 640 spectrophotometer was used, and measurements collected in the wavelength range from 400 to 1100 nm. Special care was made to deconvolve the signal from the alumina substrate from the signal due to the nanotubes by measuring the transmission signal from each blank substrate before laying down the nanotube film and measuring the transmission of the film plus the filter. Films of various thickness (and therefore various sheet resistances) were made by the same vacuum filtration method as described previously. The transmittance of the films at 550 nm vs the sheet resistance is plotted in Figure 3. Our data are in good agreement with Manohar et al.,[20] where a transmittance of 85% is measured for $R_{\square} = 1000$ ohms/sq.

Equation 3[30] models the transparency T of a thin metallic film in air, assuming that the film thickness is much less than the wavelength (in our case films are on the order of 10−20 nm thick and optical wavelengths are around 550 nm):

$$T = \frac{1}{\left(1 + \frac{2\pi}{c}\sigma_{ac}d\right)^2} = \frac{1}{\left(1 + \frac{2\pi}{c\,R_{\square dc}}\frac{\sigma_{ac}}{\sigma_{dc}}\right)^2} \tag{3}$$

Here, σ_{dc} is the DC conductivity, σ_{ac} is the optical conductivity, and d is the film thickness. We assume σ_{ac}/σ_{dc} remains constant for NTNs of different densities in the measured

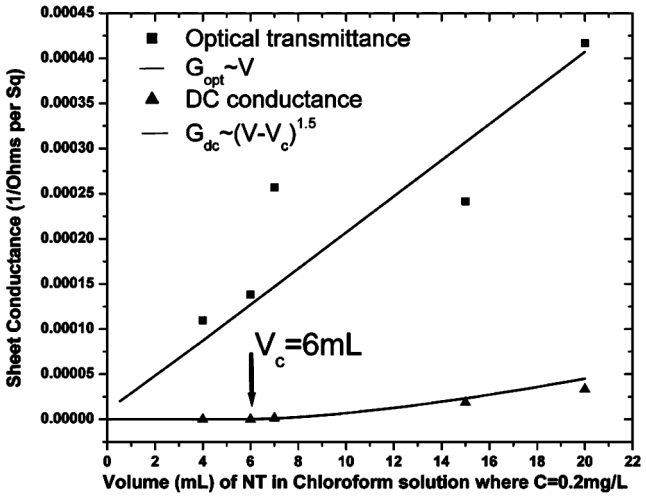

Figure 4. DC and optical sheet conductance at 800 nm vs volume of NT solution. The optical conductance was calculated using eq 3 from the measured transmitted power at 800 nm. The arrow indicates the DC percolation threshold. The optical conductance is proportional to nanotube density.

optical frequency range. By plotting $R_{\square dc}$ vs T and fitting the data to eq 3, one can estimate the value of σ_{ac}/σ_{dc}. We find that $\sigma_{ac} = \sigma_{dc}$ provides the best fit (see Figure 3). Ruzicka et al.[31] performed conductivity measurements on NTNs from DC to the optical spectral range and concluded that $\sigma_{ac} = 3\sigma_{dc}$ at 500 nm for their films, in broad agreement with our findings.

Notice that in Figure 3, even for rare networks (high sheet resistance), 100% transparency is not observed. To investigate this, we examine the optical conductance of NTNs that are near the DC percolation threshold. To calculate the optical conductance, eq 3 was used to convert transparency of the films at 800 nm to optical sheet conductance. Figure 4 shows a plot of the DC and optical conductance at 800 nm for nanotube densities near the percolation critical point. Notice that percolation issues do not arise for optical transparency, as this parameter is determined by the on-tube excitations and not on the intertube conductance. In fact, the sheet conductance in the optical frequency range is expected to be strictly proportional to the nanotube density, as observed.

It is expected that percolation issues will be important for the operation of active electronic devices with nanotube network conducting channels, such as field effect transistor devices. For a dense network, conductive nanotubes can act to screen the gate voltage, thus decreasing the on/off ratio of the device. For a rarified network, however, such screening is not an issue, and the network can serve as the source-to-drain conducting channel. Additionally, for a dense network involving both metallic and semiconducting nanotubes, the conductance of the off state, which can be reached by an application of a positive gate voltage, will be dominated by the conductance of the metallic tubes. Assuming the same conductance for metallic and negatively biased semiconducting nanotubes, a ratio of the metallic to semiconducting tubes of 1 to 2 would suggest a modulation (on/off conductance ratio) of 3. This ratio can of course be increased if imperfections lead to nonconducting (or poorly conducting) metallic nanotubes, or if metallic tubes are eliminated through ohmic annealing. However, in rarefied networks, percolation issues can also tend to increase the on/off ratio. For a sample with very few pathways from source to drain, there is a high probability that there will exist no continuous all-metallic tube paths, therefore yielding a negligible off current, and an on/off ratio several orders of magnitude higher than the on/off ratio for a thick film.

The nanotube network architecture, in addition to being flexible and conductive, is a transparent medium, opening up new application opportunities. Concerning the optical transparency of NTNs in the visible spectral range, our experiments indicate that the parameters important for applications are close to, but nevertheless below, ITO, which is the standard material used in transparent conducting material applications. Significant improvements are expected, however, with appropriate materials optimization. The overall conductance is limited by the intertube resistance of 100 MΩ, about 4 orders of magnitude larger that the resistance of the tube themselves, 10 kΩ. The same ratio is obtained if one compares the mobility of single nanotubes (100 000 cm^2/Vs) with that of networks (between 10 and 100 cm^2/Vs). Reducing the intratube resistance therefore appears to be the primary avenue for increasing device performance.

Acknowledgment. We acknowledge the NSF IGERT: Materials Creation Training Program (MCTP) − DGE−0114443 for equipment and supplies. This work was also supported by NSF grant 0404029.

References

(1) Duerkop, T.; Getty, S.; Cobas, E.; Fuhrer, M. *Nano Lett*. **2004**, *4*, 35.
(2) Yao, Z.; Kane, C. L.; Dekker, C. *Phys. Rev. Lett*. **2000**, *84*, 2941.
(3) Javey, A.; Kim, H.; Brink, M.; Wang, Q.; Ural, A.; Guo, J.; McIntyre, P.; McEuen, P.; Lundstrom, M.; Dai, H. J. *Nature Mater*. **2002**, *1*, 241.
(4) Meitl, M.; Zhou, Y.; Gaur, A.; Jeon, S.; Usrey, M.; Strano, M.; Rogers, J. *Nano Lett*. **2004**, *4*, 1643.
(5) Shiraishi, M.; Takenobu, T.; Iwai, T.; Iwasa, Y.; Kataura, H.; Ata, M. *Chem. Phys. Lett*. **2004**, *394*, 110.
(6) Zhou, Y.; Gaur, A.; Hur, S.; Kocabas, C.; Meitl, M.; Shim, M.; Rogers, J. *Nano Lett*. **2004**, in press.
(7) Wu, Z.; Chen, Z.; Du, X.; Logan, J.; Sippel, J.; Nikolou, M.; Kamaras, K.; Reynolds, J.; Tanner, D.; Hebard, A.; Rinzler, A. *Science* **2004**, *305*, 1273.
(8) Li, Z.; Dharap, P.; Nagarajaiah, S.; Barrera, E.; Kim, J. *Adv. Mater*. **2004**, *16*, 640.
(9) Abraham, J.; Philip, B.; Witchurch, A.; Varadan, V.; Reddy, C. *Smart Mater. Struct. 2004*, *13*, 1045.
(10) Kuttel, O.; Groening, O.; Emmenegger, C.; Schlapbach, L. *Appl. Phys. Lett*. **1998**, *73*, 2113.
(11) Lim, S.; Jeong, H.; Park, Y.; Bae, D.; Choi, Y.; Shin, Y.; Kim, W.; An, K.; Lee, Y. J. *Vac. Sci. Technol. A* **2001**, *19*, 1786.
(12) Bradley, K.; Gabriel, J. C.; Gruner, G. *Nano Lett*. **2003**, *3*, 1353.
(13) Lay, M. D.; Novak, J. P.; Snow, E. S. *Nano Lett*. **2004**, *4*, 603.
(14) Pike, G. E.; Seager, C. *Phys. Rev. B* **1974**, *10*, 1421.
(15) Yi, Y.; Sastry, A. *Phys. Rev. E* **2002**, *66*, 066130.
(16) Kirkpatrick, S. *Rev. Mod. Phys*. **1973**, *45*, 574.
(17) Ounaies, Z.; Park, C.; Wise, K.; Siochi, E.; Harrison, J. *Compos. Sci. Technol*. **2003**, *63* 1637.
(18) Barrau, S.; Demont, P.; Peigney, A.; Laurent, C.; Lacabanne, C. *Macromolecules* **2003**, *36*, 5187.
(19) Coleman, J.; Curran, S.; Dalton, A.; Davey, A.; McCarthy, B.; Blau, W.; Barklie, R. *Phys. Rev. B* **1998**, *58*, 7492.

(20) Saran, N.; Parikh, K.; Suh, D.; Munoz, E.; Kolla, H.; Manohar, S. *J. Am. Chem. Soc.* **2004**, *126*, 4462.
(21) Sreekumar, T.; Liu, T.; Kumar, S.; Ericson, L.; Hauge, R.; Smalley, R. *Chem. Mater.* **2003**, *15*, 175.
(22) Armitage, N. P.; Gabriel, J.; Gruner, G. *J. Appl. Phys.* **2004**, *95*, 3228.
(23) Spotnitz, M.; Ryan, D.; Stone, H. J. *Mater. Chem.* **2004**, *14*, 1299.
(24) Kim, Y.; Minami, N.; Zhu, W.; Kazaoui, S.; Azumi, R.; Matsumoto, M. *Jpn. J. Appl. Phys.* **2003**, *42*, 7629.
(25) Xin, H.; Woolley, A. T. *Nano Lett.* **2004**, *4*, 1481.
(26) Stauffer, G. *Introduction to Percolation Theory*; Taylor & Francis: London, 1985.
(27) Stadermann, M.; Papadakis, S. J.; Falvo, M. R.; Novak, J.; Snow, E.; Fu, Q.; Liu, J.; Fridman, Y.; Boland, J. J.; Superfin, R.; Washburn, S. *Phys. Rev. B* **2004**, *69*, 201402.
(28) Sandler J.; Kirk, J.; Kinloch, I.; Shaffer, M.; Windle, A. *Polymer* **2003**, *44*, 5893.
(29) Kim, B.; Lee, J.; Yu, I. *J. Appl. Phys.* **2003**, *94*, 6724.
(30) Dressel, M.; Gruner; *G. Electrodynamics of Solids: Optical Properties of Electrons in Matter*; Cambridge University Press: Cambridge, 2002.
(31) Ruzicka, B.; Degiorgi, L.; Gaal, R.; Thien-Nga, L.; Bacsa, R.; Salvetat, J.; Forro, L. *Phys. Rev. B* **2000**, *61*, 2468.

NL048435Y